Instrumentation and Measurement
Technology Conference - IMTC 2007
Warsaw, Poland, May 1-3, 2007

System Identification Approach Applied to Drift Estimation.

Frans Verbeyst[1,2], Rik Pintelon[1], Yves Rolain[1], Johan Schoukens[1] and Tracy S. Clement[3]
[1]Department ELEC, Vrije Universiteit Brussel, Pleinlaan 2, B-1050 Brussels, Belgium, rik.pintelon@vub.ac.be
[2]NMDG Engineering, C. Van Kerckhovenstraat 110, B-2880 Bornem, Belgium, frans.verbeyst@nmdg.be
[3]National Institute of Standards and Technology, Boulder, CO 80305 USA, clementt@boulder.nist.gov

Abstract - *A system identification approach is applied to estimate the time base drift introduced by a high-frequency sampling oscilloscope. First, a new least squares estimator is proposed to estimate the delay of a set of repeated measurements in the presence of additive and jitter noise. Next, the effect of both additive and jitter noise is studied in the frequency domain using simulations. Special attention is devoted to the covariance matrix of the experiments, which is used to construct a weighted least squares estimator that minimizes the uncertainty of the estimated delays. Comparative results with respect to other state-of-the-art methods are shown. Finally, the enhanced method is applied to estimate the drift observed in repeated impulse response measurements of an opto-electrical converter using an Agilent 83480A sampling oscilloscope in combination with a 83484A 50 GHz electrical plug-in.*

Keywords - *large-signal network analysis, sampling oscilloscopes, system identification, time base drift, time base jitter.*

I. INTRODUCTION

In order for large-signal network analyzers [1],[2] to accurately measure the voltage and current at both ports of a high-frequency nonlinear device, additional calibration is required compared to classical vector network analyzers. On top of the relative calibration, an absolute power and phase calibration are needed: the amplitude and phase at one frequency must be related to those at other frequencies. The power calibration is performed using a calibrated power sensor. The phase calibration is performed using an harmonic phase reference, which is essentially a pulse generator. This one is calibrated using a high-frequency sampling oscilloscope, which itself requires calibration because it suffers from both time base errors and voltage resolution errors. The non-ideal amplitude and phase characteristic of the scope is estimated using either a nose-to-nose calibration technique [3],[4] or by measuring the impulse response of a photodiode which is calibrated using an electro-optic sampling (EOS) system [5]. Both techniques require that one properly deals with the time base errors.

One of these time base errors is referred to as time base drift. When collecting a large number of repeated measurement records of the impulse response of a linear time-invariant system using a high-frequency sampling oscilloscope, it was found that the successive measurements slightly shift over time, within the acquisition window. As such it is essential to compensate for this drift before averaging.

This paper describes a system identification approach to estimate the time base drift introduced by a high-frequency sampling oscilloscope in the presence of additive noise and jitter. The estimations are performed in the frequency domain.

The initial method uses the first measurement record as a reference signal during the alignment of successive measurements. This paper however focusses on a new least squares estimator, which uses the aligned average as a reference signal instead of the first measurement. The resulting "enhanced LS" estimator clearly outperforms the initial estimator when the additive noise is dominant.

Next, special attention is devoted to the covariance matrix of the disturbing noise. The use of this matrix allows one to come up with a good estimate of the uncertainty on the estimated delays that describe the time base drift. Using the covariance matrix, a weighted version of the "enhanced LS" estimator is implemented that minimizes the uncertainty on the estimated delays. Furthermore, it allows to compare the expected value of the cost to the actual value of the cost and as such allows to detect model errors.

Comparative results with respect to other state-of-the-art methods are based on simulations performed in [6] and demonstrate the potential of the proposed estimators.

Finally, the enhanced method is applied to estimate the drift during repeated measurements performed at the National Institute of Standards and Technology (NIST). The impulse response of a calibrated photodiode is measured using an Agilent 83480A sampling oscilloscope in combination with a 83484A 50 GHz electrical plug-in[1]. It is shown that taking the covariance matrix into account, the uncertainty on the estimated delays can be reduced by a factor of 2.

II. PROPOSED APPROACH

Time base drift is due to imperfections on the position of the trigger point relative to the signal and results in a time shift of the signal in the acquisition window. As a result, successive measurements correspond to delayed versions of

1. Trade names are used only to adequately specify the experimental conditions. This does not constitute an endorsement by the National Institute of Standards and Technology. Other products may perform as well or better.

the "exact" signal. In our approach, the delay τ_k models this effect and varies with respect to the realization index k. The resulting signal model is

$$y_k(t_i) = y_0(t_i + n_t(k, t_i) + \tau_k) + n_y(k, t_i). \quad (1)$$

Herein, $y_k(t_i)$ represents the k-th measurement of the true but unknown signal $y_0(t_i)$ when both additive noise $n_y(k, t_i)$ and jitter $n_t(k, t_i)$ are added as a part of the measurement. Both noise sources are assumed to be zero mean, normally distributed, independent and stationary with respect to t, and as a result they are also independent with respect to realization index k. Furthermore, it is assumed that $t_i = i\Delta t$, where Δt represents the sampling period. In this paper, $\sigma^2_{n_y}$ represents the variance of the additive noise and $\sigma^2_{n_t}$ is the variance of the jitter noise.

Let $Y_k(\omega_m)$ correspond to the discrete Fourier transform of $y_k(t_i)$. First, the time base drift of each acquisition is estimated using the first acquisition as a reference signal. This is referred to as the "naive LS" estimator, which minimizes the cost function V_{LS_k} via the frequency domain, taking M spectral components into account.

$$V_{LS_k} = \sum_{m=1}^{M} \left| Y_k(\omega_m) - e^{-j\omega_m\tau_k} \cdot Y_1(\omega_m) \right|^2, \; k = 2 \,..\, K \quad (2)$$

Next, the true but unknown signal is used as the reference signal. The resulting "enhanced LS" cost function then becomes

$$V_{LS} = \sum_{k=1}^{K} \sum_{m=1}^{M} \left| Y_k(\omega_m) - e^{-j\omega_m\tau_k} \cdot Y_0(\omega_m) \right|^2. \quad (3)$$

Since the spectrum $Y_0(\omega_m)$ appears linearly in the equation error, it is possible to eliminate it from the cost. Thus, the cost function becomes a function of the unknown delays $\theta = \left[\tau_1 \,..\, \tau_K\right]^T$ only and is estimated via the frequency domain:

$$V_{LS}(\theta) = \sum_{k,m} \left| Y_k(\omega_m) \cdot e^{j\omega_m\tau_k} - \frac{1}{K} \sum_{l=1}^{K} Y_l(\omega_m) \cdot e^{j\omega_m\tau_l} \right|^2 \quad (4)$$

It is possible to introduce an arbitrary delay τ as follows

$$Y_k(\omega) = e^{-j\omega(\tau_k + \tau)} \cdot [Y_0(\omega) \cdot e^{j\omega\tau}], \; k = 1 \,..\, K, \quad (5)$$

without influencing $V_{LS}(\theta)$. If $\tilde{Y}_0(\omega) = Y_0(\omega) \cdot e^{j\omega\tau}$ is considered to be the new reference, it is clear that there is a degeneracy: (only) one delay can be freely chosen. One possibility is to select one delay to be zero. Here, τ_1 is set to zero.

The derivatives of (4) with respect to τ_2 up to τ_K yield the gradient while the second derivatives yield the Hessian of the cost. The Newton-Raphson iteration scheme is then used to find the estimates $\tau_2, .., \tau_K$ which minimize (4), given that $\tau_1 = 0$. Starting values are readily available from the naive LS estimator (2).

Although these starting values reduce the number of iterations that are needed to converge to the solution, it was found that zero starting values also do the job. Even starting values where the sign of the delay is incorrect still lead to convergence to the same solution. This shows the robustness of the method to poor starting values.

III. ANALYSIS OF THE NOISE SOURCES

The assumption of circular complex noise in the frequency domain is only valid in the case of additive noise. As soon as jitter is present, this assumption is no longer valid. The impacted frequency range depends on the actual signal being measured.

This is demonstrated based on simulations which are kept as realistic as possible, using the analytical expression which can be found in [7]. The jitter noise $n_y(k, t_i)$ is assumed to be zero mean, normally distributed, independent and stationary with respect to t. Its standard deviation is assumed to be known and is set equal to 1 ps. The additive noise is set to zero.

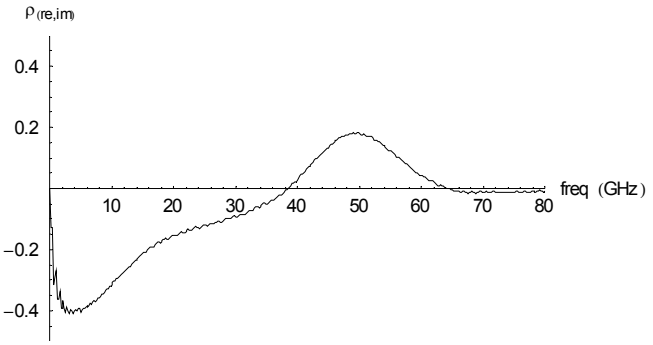

Figure 1. Correlation coefficient of the real and the imaginary part of the Fourier transform of the 5000 realizations of the impulse response.

Calculating the sample variance of the real and imaginary part of the spectral data corresponding to 5000 realizations of

the simulation data, it becomes clear that although the sum of the variances of the real and imaginary part is constant as a function of frequency, this is not the case for the real part and the imaginary part. Figure 1 shows the correlation coefficient of the real and imaginary part of the spectral data, indicating correlation up to 65 GHz.

Furthermore, one can take a look at the correlation between spectral contributions originating from different frequencies (real, real), (real, imag), (imag, real) and (imag, imag). Correlation is observed up to about 130 GHz.

IV. CALCULATION OF THE NOISE COVARIANCE MATRIX

Next, it is shown that it is possible to calculate the covariance matrix in the frequency domain, if one has an estimate of the sample variance in the time domain [7].

Because the noise is not circular complex as soon as jitter is present, the frequency covariance matrix must take into account the real and the imaginary parts of the spectrum separately. Given the noisy measurement $y(t)$ and its Fourier transform $Y(\omega)$, the covariance matrix in the frequency domain can then be calculated using (6), provided that the real and the imaginary parts are separated.

$$Cov[Y(\omega)] = J \cdot Cov\,[y(t)] \cdot J^{T} \tag{6}$$

In (6), J^{T} represents the transpose of the Jacobian matrix $J \in \mathbb{R}^{2M \times N}$, which is the matrix notation of the discrete Fourier transform where the odd rows correspond to the real part and the even rows to the imaginary part of the Fourier coefficient. M represents the number of frequency components of interest and N is the number of time points of one measurement of the impulse response. The covariance matrix in the time domain $Cov[y(t)] \in \mathbb{R}^{N \times N}$ reduces to a diagonal matrix in case the jitter is independently distributed over time. The values on this diagonal correspond to the variance as a function of time.

Figure 2 is the equivalent of figure 1, but is now calculated using (6) where the variance is known as a function of time. Both show excellent correspondence.

Now it is possible to construct a weighted least squares estimator which minimizes the uncertainty on the estimated delays and, at the same time, has a known expected value of the cost function, such that the obtained cost function can be compared to its expected value. This criterion can then be used to detect model errors.

$$V_{WLS} = e^{T}(\tau) \cdot [Cov(Y(\omega))]^{-1} \cdot e(\tau),\ e = \left[e_1 \,..\, e_K\right]^{T} \tag{7}$$

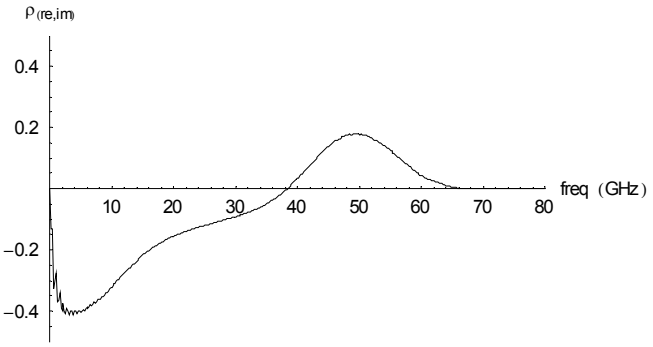

Figure 2. Correlation coefficient of the real and the imaginary part using (6).

$$e_k = \left[re(e_{k,1})\ im(e_{k,1})\ ..\ re(e_{k,M})\ im(e_{k,M})\right] \tag{8}$$

$$e_{k,m} = Y_k(\omega_m) \cdot e^{j\omega_m \tau_k} - \frac{1}{K} \sum_{l=1}^{K} Y_l(\omega_m) \cdot e^{j\omega_m \tau_l} \tag{9}$$

The advantages of this method will become apparent when it will be applied to both simulations and measurements.

Using the Gauss-Newton method to minimize (7) is somewhat challenging because it requires the Jacobian

$$J = \frac{\partial e(\tau)}{\partial \tau} \in \mathbb{R}^{K \cdot 2M \times (K-1)}. \tag{10}$$

Typical values for both K and M in an experimental environment are 500. This results in a large Jacobian matrix of size 500000×499 and a covariance matrix of 1000×1000. Fortunately, there is some structure in the Jacobian matrix derived from (9), such that the problem can be solved in blocks of size $2M \times (K-1)$.

V. SIMULATIONS

A first set of simulations is used to verify the correctness of the implementations and the performance of each estimator. The simulations are based on the same analytical expression of the impulse response as the one used in [7]. The drift is estimated in the presence of both additive and jitter noise, where both are set to have realistic values: both are Gaussian, zero mean with a standard deviation of respectively 0.6 mV and 1 ps. The exact signal is assumed to be known and [7] can be used to calculate the variance as a function of time. As such (6) can be used to calculate $Cov[Y(\omega)]$.

Each simulation consists of 500 realizations of the signal. Hence, $K = 500$. Each realization contains 4096 time samples of the impulse response, which spans an acquisition window of 5 ns. If spectral components are taken into account

up to 100 GHz, then $M = 500$.

Comparative results are shown for two situations.

A. Zero drift

During the first simulation, the drift is set to be exactly zero. Due to the jitter noise and the additive noise, the estimated drift becomes a stochastical variable, which is not exactly zero. Because of the degeneracy (5), only the standard deviation is shown in Table 1.

Table 1. Uncertainty of the estimated drift τ (case where the exact drift is zero).

Estimator	Uncertainty σ_τ (ps)	95% confidence interval (ps) of σ_τ
naive LS	0.260	0.245 .. 0.277
enhanced LS	0.253	0.238 .. 0.270
enhanced WLS	0.132	0.124 .. 0.141

Table 1 clearly shows that the naive LS estimator (2) performs equally well as the enhanced LS estimator (4), while the enhanced WLS estimator (7) reduces the uncertainty on the estimated delay by as much as a factor 2.

Furthermore, when overlooking the fact that, in the presence of jitter, the noise in the frequency domain is no longer circular complex, the uncertainty on the estimated delay for the enhanced LS estimator is underestimated by a factor of more than 10 when extracted from the parameter covariance matrix. Using the full covariance matrix (6), the estimated uncertainty on the delay turns out to be 0.242 ps and falls within the 95% confidence interval of the obtained uncertainty.

Finally, it is important to notice that in the case of the enhanced WLS estimator, the expected value of the cost is 499500 ± 1999. The realized cost turns out to be 497250 and falls just outside the 95% confidence interval of the expected value of the cost, indicating that no significant model errors can be detected, given the noise level used during simulation.

B. Linear drift

Similar results and ditto conclusions can be drawn when the drift is known to be a linear function of the realization index. Applying a delay of 0.01 ps per realization, the drift of the first realization is zero, while that of the 500th realization is known to be 4.99 ps.

This time the actual value of the cost of the WLS estimator turns out to be 498240 and is well within the 95% confidence interval of the expected value of the cost.

The general conclusion of these simulations is that in realistic situations, corresponding to the nose-to-nose and EOS-based measurements, the effect of using the aligned average instead of the first realization as a reference signal is expected to be minimal. However, using proper weigthing based on the full covariance matrix of the measurements has significant impact.

VI. COMPARISON TO OTHER STATE-OF-THE-ART METHODS

Next the performance of the implemented estimators is compared to the two most relevant estimators described in [6]. The comparison is based on the simulated signal that is described in Appendix I of [6].

Figure 3 shows the noise-free signal, where both the time and amplitude are given in arbitrary units. In fact, the time scale is expressed in integer multiples of the sampling period Δt.

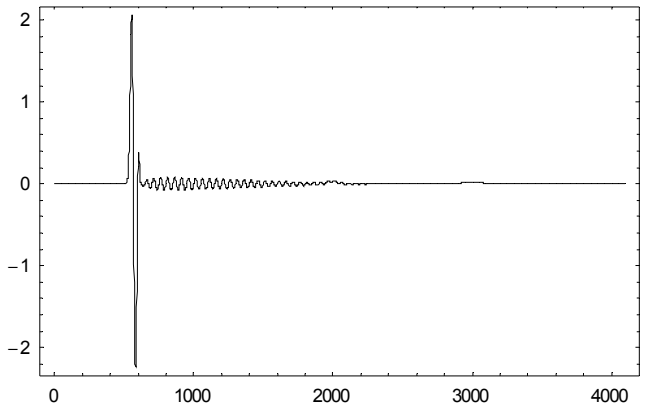

Figure 3. Noise-free simulated signal as described in [6] (both axes in arbitrary units).

The "naive cross-correlation" method described by [6] can be compared to the naive LS estimator (2) described in this paper, because both use the first realization as a reference signal. However, the method described in [6] is based on a cross-correlation technique performed in the time domain and as such restricted to a grid corresponding to integer multiples of Δt. In order to overcome this limitation, [6] searches for the global minimum about the grid value which maximizes the cross-correlation based on a "golden search and parabolic interpolation".

The "complete cross-correlation" method proposed by [6] calculates the relative drift between any combination of the K realizations to come up with an averaged drift of all realizations with respect to the first realization. As such, this method is similar to the enhanced LS estimator (3) described in this paper.

Comparisons are performed for different relevant situations, which are summarized in Table 2.

For each of the above situations, a set of 100 misaligned signals are generated. The standard deviation of the random drift associated with each signal is set to 2.5. In fact the value of σ_{n_y} should be compared to a peak-to-peak value of about 4.2, while both σ_{n_t} and the random drift are expressed as multiples of Δt.

In order to get an idea of what is meant by "moderate"

Table 2. Selected values of σ_{n_t} and σ_{n_y} (in arbitrary units).

Situation	σ_{n_t}	σ_{n_y}
no jitter, small additive noise	0	0.02
no jitter, moderate additive noise	0	0.1
significant jitter, moderate additive noise	3	0.1
moderate jitter, small additive noise	1	0.02
moderate jitter, moderate additive noise	1	0.1

jitter $\sigma_{n_t} = 1$ and "moderate" additive noise $\sigma_{n_y} = 0.1$, figure 4 shows one realization of such a noisy signal while zooming in to the main portion of the pulse.

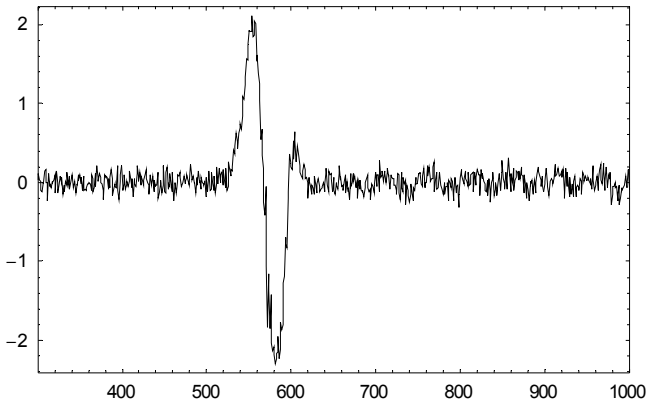

Figure 4. Zoomed version of the simulated signal in the case of moderate jitter and moderate additive noise (both axes in arbitrary units).

The simulations show that the naive LS method clearly outperforms the naive cross-correlation method described in [6]. It is believed that this is due to the fact that the latter suffers from interpolation problems. Indeed, an interpolation technique is required to increase the time resolution to a value that is smaller than Δt, and this may cause problems in the presence of noise.

Table 3 shows the results of the simulations in the case of dominant jitter noise. Both the naive LS method (2), the enhanced LS method (3) and the complete cross-correlation method [6] perform equally well. The enhanced WLS method (7) reduces the RMS prediction error by as much as a factor of 2 and clearly outperforms all other methods altogether.

The most important improvement of the WLS method is that it allows to compare the expected value of the cost to the realized value of the cost and as such allows to detect model errors or anomalies in the measurements. Based on 100 realizations and 500 spectral component, the expected value of the cost is 99900 ± 894. The realized cost turns out to be 99525 and falls within the 95% confidence interval. Hence, it can be concluded that there are no detectable model errors, given the noise levels used during simulation. The other methods provide no information to the user to draw such conclusions.

Table 3. RMS prediction error for the simulation where $\sigma_{n_t} = 1$ and $\sigma_{n_y} = 0.02$.

Estimator	RMS prediction error	95% confidence interval
naive cross-correlation	~0.25	
complete cross-correlation	~0.15	
naive LS	0.16	0.14 .. 0.19
enhanced LS	0.16	0.14 .. 0.19
enhanced WLS	0.08	0.07 .. 0.09

Table 4 shows the results of the simulations in the case of both moderate jitter and moderate additive noise. In this case, the performance of the naive LS method equals that of the complete cross-correlation method and is significantly better than the naive cross-correlation method. Again, the enhanced WLS method has the best performance. However, the improvement with respect to the enhanced LS method is rather limited. This is due to the fact that the jitter noise is no longer dominant, as it was the case for the simulations corresponding to Table 3. The enhanced LS method in its turn shows a limited improvement over the naive LS method.

Table 4. RMS prediction error for the simulation where $\sigma_{n_t} = 1$ and $\sigma_{n_y} = 0.1$.

Estimator	RMS prediction error	95% confidence interval
naive cross-correlation	~0.60	
complete cross-correlation	~0.22	
naive LS	0.21	0.18 .. 0.24
enhanced LS	0.18	0.16 .. 0.21
enhanced WLS	0.16	0.14 .. 0.19

VII. MEASUREMENT RESULTS

The 500 repeated impulse response measurements of a calibrated photodiode were performed at NIST using an Agilent 83480A sampling oscilloscope in combination with a 83484A 50 GHz electrical plug-in. The block diagram of the required measurement setup is shown in figure 5.

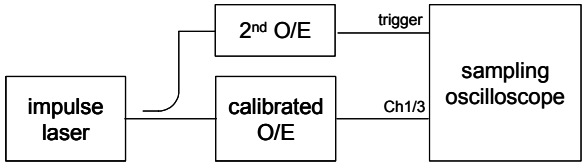

Figure 5. Setup used during the impulse response measurement.

Figure 6 zooms into the main portion of one impulse response measurement. Figure 7 plots all 500 measurements on top of each other, clearly demonstrating the drift.

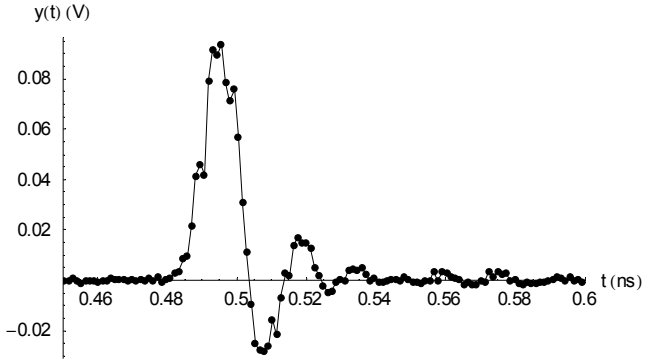

Figure 6. Main portion of the first impulse response measurement.

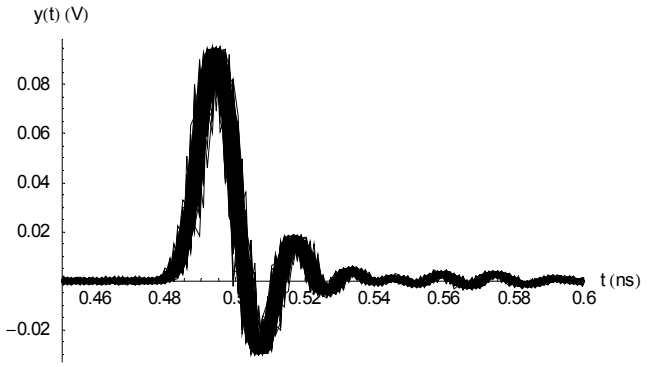

Figure 7. Main portion of all impulse response measurements.

The drift is estimated using the naive LS method (2) and the enhanced LS method (3). Although there is some difference, the difference is rather limited.

When the full covariance matrix based on the estimated jitter and additive noise standard deviation is used to construct the WLS estimator (7), figure 8 shows a significantly smoother characteristic, resulting from a decreased uncertainty on the estimated drift. This is an expected property of the WLS, and is due to the use of a proper weighting of the frequency components in the cost function.

These results are consistent with those of the simulations above, where both the additive noise and the jitter noise are moderate, but where the latter is dominant.

This also motivates the smoothing of the estimated time base drift during the estimation of the time base jitter [7].

VIII. CONCLUSIONS

Using system identification techniques, it is possible to derive an estimate of time base drift in the presence of both additive and jitter noise. Due to the identification framework, the properties of this estimator are well understood, and this can be used to verify the quality of the measurements. To the knowledge of the authors, the proposed method performs

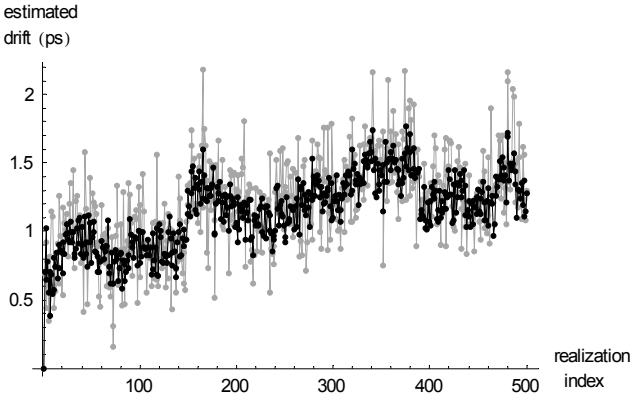

Figure 8. Comparison of the estimated drift by use of the enhanced LS method (connected gray dots) and the enhanced WLS method (connected black dots) for the 500 realizations.

better than any other published technique.

The use of a proper weighting of the contribution of the individual spectral components to the cost function not only provides a relevant value for the cost function. It also reduces the uncertainty on the estimated drifts in the presence of a realistic quantity of additive and jitter noise by as much as a factor of 2. The weighting is based on the full covariance matrix, where the contributions of the real and the imaginary part are separately taken into account.

IX. ACKNOWLEDGEMENT

The authors thank Paul Hale and Dylan Williams for their support.

X. REFERENCES

[1] T. Van den Broeck, J. Verspecht, “Calibrated Vectorial Nonlinear Network Analyzers,” IMS Conference Proceedings, pp. 1069-1072, May 1994, USA.

[2] M. Vanden Bossche, “A Network Analyzer for Complete Active Component Characterization and Real-Time Harmonic Load Pull,” CAD, Test and Measurement Supplement of Microwave Journal, November 2004.

[3] J. Verspecht, K. Rush, “Individual Characterization of Broadband Sampling Oscilloscopes with a 'Nose-to-Nose' Calibration Procedure,” IEEE Transactions on Instrumentation and Measurement, Vol. 43, No. 2, pp. 347-354, April 1994.

[4] P. Hale, T. Clement, K. Coakley, C. Wand, D. DeGroot and A. Verdoni, “Estimating the Magnitude and Phase Response of a 50 GHz Sampling Oscilloscope Using the “Nose-To-Nose” Method,”, 55th ARFTG Conf. Digest, pp. 35-42, June 2000.

[5] D. Williams, P. Hale, T. Clement, and J. Morgan, "Calibrating electro-optic sampling systems," Int. Microwave Symposium Digest, Phoenix, AZ, pp. 1527-1530, May 20-25, 2001.

[6] K. Coakley and P. Hale, “Alignment of Noisy Signals,” IEEE Transactions on Instrumentation and Measurement, Vol. 50, No. 1, pp. 141-149, February 2001.

[7] F. Verbeyst, Y. Rolain, J. Schoukens, R. Pintelon, “System Identification Approach Applied to Jitter Estimation”, IMTC Conference Proceedings, pp. 1752-1757, winner of a "Honorable mention recognized by the Award Commission of Agilent Technologies", IMTC ‘06, April 2006, Sorrento, Italy.